

Single particle relaxation time versus transport scattering time in a 2D graphene layer

E. H. Hwang and S. Das Sarma
*Condensed Matter Theory Center, Department of Physics,
 University of Maryland, College Park, MD 20742-4111*
 (Dated: November 26, 2024)

We theoretically calculate and compare the single-particle relaxation time (τ_s) defining quantum level broadening and the transport scattering time (τ_t) defining Drude conductivity in 2D graphene layers in the presence of screened charged impurities scattering and short-range defect scattering. We find that the ratio τ_t/τ_s increases strongly with increasing $k_F z_i$ and κ where k_F , z_i , and κ are respectively the Fermi wave vector, the separation of the substrate charged impurities from the graphene layer, and the background lattice dielectric constant. A critical quantitative comparison of the τ_t/τ_s results for graphene with the corresponding modulation-doped semiconductor structures is provided, showing significant differences between these two 2D carrier systems.

PACS numbers: 81.05.Uw; 72.10.-d, 72.15.Lh, 72.20.Dp

I. INTRODUCTION AND BACKGROUND

In an impure disordered conductor (either a metal or a doped semiconductor) scattering by static impurities and defects, in general, leads to two distinct momentum relaxation times; the scattering life time or the transport relaxation time (denoted by τ_t in this paper, but often just called τ) and the quantum lifetime or the single-particle relaxation time (denoted by τ_s in this paper, but often also called τ_q). Although τ_t and τ_s both arise from impurity scattering in the metallic regime, they are in general distinct and unique with no direct analytical relationship connecting them, except for the simple (and often unrealistic) model of completely isotropic s -wave zero-range impurity scattering when they are equal. In particular, τ_t determines the conductivity, $\sigma = ne\mu \propto \tau_t$ where n is the carrier density and μ the mobility, whereas τ_s determines the quantum level broadening, $\Gamma \equiv \hbar/2\tau_s$, of the momentum eigenstates (i.e. the band states defined by a momentum $\hbar\mathbf{k}$ with \mathbf{k} as the conserved wave vector). The difference between τ_t and τ_s arises from the subtle effect of the wave vector dependent impurity potential $u_i(\mathbf{k})$ which distinguishes between momentum scattering in *all* directions contributing to τ_s^{-1} and transport relaxation τ_t^{-1} which is unaffected by forward scattering (or more generally, small-angle scattering)¹.

In this paper we study theoretically τ_t and τ_s in the 2D graphene layer due to long-range and short-range impurity scattering, finding interesting behavior in the ratio τ_t/τ_s as a function of impurity location, carrier density, and the system environment (e.g. the background lattice dielectric constant of the substrate). We compare graphene τ_t/τ_s with the corresponding situation in the extensively studied 2D semiconductor systems, finding significant difference.

In 3D metals or semiconductors, the effective impurity-electron interaction potential is almost always short-ranged. This is true even when the bare impurity potential is long-range Coulombic since carrier-induced electronic screening of the charged impurities is highly effective. This strongly screened short-range impurity poten-

tial in 3D systems (as well as in 2D systems when electrons and impurities are not spatially separated) has led to the almost universal theoretical adoption of the uncorrelated white-noise zero-range impurity potential model for studying the impurity scattering effect on “metallic” transport properties. Since such a white-noise disorder, by definition, leads to isotropic impurity scattering dominated entirely by large-angle scattering, $\tau_t = \tau_s$ in ordinary metals and semiconductors for such a zero-range disorder model as forward scattering simply plays no special role here. Graphene is, however, qualitatively different even for this short-range white noise disorder model due to its chiral sublattice symmetry which suppresses backward (i.e. a scattering induced wave vector change by $2k_F$ from $+k_F$ to $-k_F$) scattering², thus introducing an intrinsic chiral preference for forward scattering over backward scattering. As we show later in this paper, due to this suppression of backward scattering, the zero-range white-noise disorder potential model leads to $\tau_t = 2\tau_s$ in graphene in contrast to the $\tau_t = \tau_s$ in ordinary metals and semiconductors. This is due to the importance of k_F (rather than $2k_F$) scattering in dominating graphene transport properties whereas the small-angle scattering always dominates τ_s .

For long-range impurity scattering, however, it has been shown¹ that τ_t can exceed τ_s by a large factor, and in high-mobility 2D modulation-doped semiconductor structures, where the predominant scattering is the small-angle scattering due to charged impurities located far from the 2D electron layer, in general $\tau_t \gg \tau_s$. In this paper, we theoretically calculate τ_t/τ_s (as well as τ_t and τ_s individually) for 2D graphene electrons (and holes) due to both long-range and short-range impurity scattering, taking into account the dependence on the impurity location. We find that there are significant differences between 2D graphene (with its linear chiral dispersion) and 2D semiconductors, showing that τ_t/τ_s in general could also be very large for graphene although the behavior is quite different from the corresponding 2D semiconductors.

Our work is restricted entirely to extrinsic or doped (or

gated) graphene where the Fermi level is away from the charge neutral Dirac point (taken to be the energy zero). There has been extensive recent theoretical work^{3,4,5,6,7} on the charged impurity scattering limited transport properties in gated extrinsic graphene, but the single-particle quantum relaxation time τ_s (and its relation to the transport scattering time τ_t) has not been discussed. We note that while τ_t has been experimentally studied recently in extrinsic graphene^{8,9} through measurements of density-dependent conductivity, the corresponding τ_s has not yet been directly experimentally measured. The most direct way of measuring τ_s experimentally is by measuring the quantum level broadening $\Gamma = \hbar/2\tau_s$ through the Dingle temperature $T_D = \Gamma/\pi k_B$. The Dingle temperature can be measured in low-field SdH magnetoresistance oscillations as has been done extensively in 2D semiconductor structures¹⁰. Any measurement of the single-particle level broadening, e.g. magnetization, also gives an estimate for τ_s . Experimental comparisons of τ_t/τ_s for various system parameters (e.g. carrier density, impurity location, materials parameters such as effective mass and lattice dielectric constant) have been carried out in semiconductor based 2D systems, but not in graphene since measurements of τ_s are unavailable in graphene. Extensive

measurements of τ_t as a function of carrier density, i.e. gate voltage, however, have been carried out^{8,9} in graphene recently.

In our theoretical calculations (and in the numerical results) we have used two complementary models of bare disorder: Long-range random charged impurity centers at or near the graphene-substrate interface and short-range model white noise disorder in the graphene layer. We also include screening (by the graphene carriers themselves) within random phase approximation (RPA) in the theory. In Sec. II we describe theoretical details and present our results. In Sec. III we discuss the relevance and significance of our theory in the context of transport experiments in gated or doped graphene, and provide a conclusion.

II. THEORY AND RESULTS

In the relaxation time approximation the graphene transport scattering time τ_t by randomly distributed impurity centers is given by^{3,6}

$$\frac{1}{\tau_t} = \frac{2\pi n_i}{\hbar} \sum_{\lambda'} \int \frac{d^2 k'}{(2\pi)^2} \frac{\langle |V_{ei}(q)|^2 \rangle}{\epsilon(q)^2} F_{\lambda\lambda'}(\mathbf{k}, \mathbf{k}') (1 - \cos \theta_{kk'}) \delta(\epsilon_{\lambda\mathbf{k}} - \epsilon_{\lambda'\mathbf{k}'}), \quad (1)$$

where n_i is the concentration of the impurity center, $q = |\mathbf{k} - \mathbf{k}'|$, $\theta_{\mathbf{k}\mathbf{k}'}$ is the scattering angle between the scattering in- and out- wave vectors \mathbf{k} and \mathbf{k}' , $\lambda, \lambda' = \pm 1$ denote the band indices, $\epsilon_{\lambda\mathbf{k}} = \lambda\gamma|\mathbf{k}|$ is a single particle energy ($\gamma = \hbar v_F$ being the graphene band velocity), and $F_{\lambda\lambda'}(\mathbf{k}, \mathbf{k}')$ is the overlap of states and given by $F_{\lambda\lambda'}(\mathbf{k}, \mathbf{k}') = (1 + \lambda\lambda' \cos \theta_{\mathbf{k},\mathbf{k}'})/2$. In Eq. (1) $V_{ei}(q)$ is the matrix elements of the scattering potential between an electron and an impurity. For charged impurities, we use the Coulomb interaction $V_{ei}(q) = 2\pi e^2/(\kappa q)$, where κ is the dielectric constant of surrounding materials, and for short-range point defect scatterers, $V_{ei}(q) = v_0$, a constant. In Eq. 1, $\epsilon(q)$ is the static RPA dielectric (screening) function appropriate for graphene¹¹, given by

$$\epsilon(q) = 1 + v_c(q)\Pi(q), \quad (2)$$

where $v_c(q) = 2\pi e^2/\kappa q$ is the electron-electron Coulomb potential, and $\Pi(q)$ is the polarizability function of graphene which is calculated to be

$$\Pi(q) = \begin{cases} 1 & \text{if } q \leq 2k_F \\ 1 + \frac{\pi q}{8k_F} - \frac{\sqrt{q^2 - 4k_F^2}}{2q} - \frac{q \sin^{-1}(2k_F/q)}{4k_F} & \text{if } q > 2k_F \end{cases}. \quad (3)$$

Since we consider elastic scattering we can neglect inter-band scattering processes ($\lambda' \neq \lambda$). Then, we have the

leading-order (in impurity disorder n_i) transport scattering time

$$\frac{1}{\tau_t} = \frac{n_i}{2\pi\hbar} \frac{E_F}{\gamma^2} \int_0^\pi d\theta \frac{\langle |V_{ei}(q)|^2 \rangle}{\epsilon(q)^2} (1 - \cos^2 \theta), \quad (4)$$

where $q = 2k_F \sin(\theta/2)$.

From a many-body-theory viewpoint the single particle relaxation time τ_s can be calculated from the electron self energy of the coupled electron-impurity system^{12,13}. The electron self-energy due to the impurity scattering is given by

$$\Sigma_\lambda(k, \omega) = \sum_{\lambda'} \frac{\langle |V_{ei}(q)|^2 \rangle}{\epsilon(q)^2} F_{\lambda\lambda'}(\mathbf{k}, \mathbf{k}') G_\lambda(\mathbf{k}', \omega), \quad (5)$$

where $G_\lambda(\mathbf{k}, \omega) = 1/(\omega - \epsilon_{\lambda\mathbf{k}} + i\delta)$ is the noninteraction Green's function. The single particle relaxation time is related to the imaginary part of the single particle self-energy function by

$$\frac{1}{\tau_s} = \frac{2}{\hbar} \text{Im} \Sigma(k_F, E_F), \quad (6)$$

with the single particle quantum (impurity induced) level broadening $\Gamma_s = \text{Im} \Sigma(k_F, E_F)$, i.e. $\tau_s = \hbar/2\Gamma_s$. In the

leading order disorder approximation, we have the single particle relaxation time τ_s

$$\frac{1}{\tau_s} = \frac{n_i}{2\pi\hbar} \frac{E_F}{\gamma^2} \int_0^\pi d\theta \frac{\langle |V_{ei}(q)|^2 \rangle}{\varepsilon(q)^2} (1 + \cos\theta). \quad (7)$$

Thus, the only difference between the scattering time τ_t [Eq. (4)] and the single-particle relaxation time τ_s [Eq. (7)] is the weighting factor $1 - \cos\theta$ in the transport scattering time. The factor $1 - \cos\theta$ weights the amount of backward scattering of the electron by the impurity. Small angle (or forward) scattering, where $\cos\theta \approx 1$, is relatively unimportant in contributing to τ_t^{-1} and contributes little to the resistivity. In normal 2D systems the factor $1 - \cos\theta$ obviously favors large angle scattering events, which are more important for the electrical resistivity. However, in graphene the large angle scattering is also suppressed due to the wave function overlap factor $1 + \cos\theta$. The transport scattering time thus gets weighted by an angular contribution factor of $(1 - \cos\theta)(1 + \cos\theta)$, which suppresses both small-angle scattering and large-angle scattering contributions in the transport scattering rate. However, the single particle relaxation time is weighted only by $1 + \cos\theta$ term. Therefore, τ_t is insensitive to both small and large angle scatterings while τ_s is only sensitive to small angle scattering events. In fact, the dominant contribution to τ_t comes from $\cos^2\theta = 0$, i.e. $\theta = \pi/2$ scattering, which is equivalent to $|\mathbf{k} - \mathbf{k}'| \equiv k_F$ “right-angle” scattering in contrast to the $2k_F$ back scattering in ordinary 2D systems. This leads to significant difference between graphene and parabolic 2D semiconductor systems with respect to the behavior of τ_t/τ_s .

Using RPA screening function [Eq. (2)] at $T = 0$ we calculate the scattering times due to charged impurities distributed completely randomly at the interface between graphene and the substrate with density n_{ic}

$$\frac{1}{\tau_{tc}} = \frac{r_s^2}{\tau_{0c}} I_{tc}(2r_s), \quad (8a)$$

$$\frac{1}{\tau_{sc}} = \frac{r_s^2}{\tau_{0c}} I_{sc}(2r_s), \quad (8b)$$

where $r_s = e^2/\gamma\kappa$ and

$$\frac{1}{\tau_{0c}} = \frac{2\sqrt{\pi}n_{ic}\gamma}{\hbar\sqrt{n}}. \quad (9)$$

In Eq. (8) $I_{tc}(x)$, $I_{sc}(x)$ are calculated to be

$$I_{tc}(x) = \frac{\pi}{2} - 2 \frac{d}{dx} [x^2 g(x)] \quad (10a)$$

$$I_{sc}(x) = -\frac{d}{dx} g(x) \quad (10b)$$

where $g(x)$ is given by

$$g(x) = -1 + \frac{\pi}{2}x + (1 - x^2)f(x) \quad (11)$$

with

$$f(x) = \begin{cases} \frac{1}{\sqrt{1-x^2}} \ln \left[\frac{1+\sqrt{1-x^2}}{x} \right] & \text{for } x < 1 \\ 1 & \text{for } x = 1 \\ \frac{1}{\sqrt{x^2-1}} \cos^{-1} \frac{1}{x} & \text{for } x > 1 \end{cases} \quad (12)$$

From Eqs. (11) and (12) we have

$$\frac{dg(x)}{dx} = \frac{\pi}{2} - \frac{1}{x} - xf(x). \quad (13)$$

The limiting forms of scattering times in the small and large r_s regimes are given by

$$\frac{\tau_{0c}}{\tau_{tc}} = \begin{cases} r_s^2 [\pi/2 + 12r_s + 8r_s \ln(r_s) + \dots] & \text{for } r_s \ll 1 \\ \pi/32 - 1/(15r_s) + O(1/r_s^2) & \text{for } r_s \gg 1 \end{cases} \quad (14)$$

and

$$\frac{\tau_{0c}}{\tau_{sc}} = \begin{cases} r_s/2 - \pi r_s^2/2 - 2r_s^3 \ln(r_s) + \dots & \text{for } r_s \ll 1 \\ \pi/16 - 1/(12r_s) + O(1/r_s^2) & \text{for } r_s \gg 1 \end{cases} \quad (15)$$

From Eq. (8) we can find easily the ratio of transport scattering time to the single particle relaxation time, τ_{tc}/τ_{sc} . Fig. 1 shows the ratio as a function of r_s . Note that the ratio is only a function of r_s and does not depend on the carrier density. We have the limiting form of τ_{tc}/τ_{sc} , in the small and large r_s regimes

$$\frac{\tau_{tc}}{\tau_{sc}} = \begin{cases} \frac{1}{\pi r_s} - \frac{16}{\pi^2} \ln(r_s) & \text{for } r_s \ll 1 \\ 2 + \frac{8}{5\pi} \frac{1}{r_s} & \text{for } r_s \gg 1 \end{cases} \quad (16)$$

For large r_s , the ratio approaches 2, which indicates that scattering is not isotropic even though the screening is strong. On the other hand, τ_{tc}/τ_{sc} diverges as $1/r_s$ for small r_s . In $r_s \rightarrow 0$ limits, where the screening is very weak, the transport scattering rate is much weaker than the single particle scattering rate, which indicates that the mobility in these limits is very high.

For short-ranged (δ -function) scatterers with impurity density $n_{i\delta}$ and potential strength v_0 we have the scattering times (considering screening effects)

$$\frac{1}{\tau_{t\delta}} = \frac{1}{\tau_{0\delta}} I_{t\delta}(2r_s) \quad (17a)$$

$$\frac{1}{\tau_{s\delta}} = \frac{1}{\tau_{0\delta}} I_{s\delta}(2r_s) \quad (17b)$$

where $1/\tau_{0\delta} = 2n_{i\delta}\sqrt{\pi}v_0^2/\sqrt{\pi}\hbar\gamma$, and $I_{t\delta}$, and $I_{s\delta}$ are given by

$$I_{t\delta}(x) = \frac{\pi}{8} - \frac{4}{3}x + \frac{3\pi}{2}x^2 - 2 \frac{d}{dx} [x^4 g(x)] \quad (18a)$$

$$I_{s\delta}(x) = \frac{\pi}{4} - \frac{d}{dx} [x^2 g(x)]. \quad (18b)$$

In Fig. 1 we show the ratio of the scattering times for the short-ranged scatterers, $\tau_{t\delta}/\tau_{s\delta}$, as a function of r_s , and the limiting forms are given by

$$\frac{\tau_{t\delta}}{\tau_{s\delta}} = \begin{cases} 2 + 32r_s \ln(r_s)/\pi & \text{for } r_s \ll 1 \\ 1 + 128r_s/105\pi & \text{for } r_s \gg 1 \end{cases} \quad (19)$$

We find that $1 \leq \tau_{t\delta}/\tau_{s\delta} \leq 2$ (see Fig. 1). The ratio does not exceed 2 for short-ranged scatterers, but for charged impurity scattering the ratio is always greater than 2. Thus the ratio of the scattering times may offer the possibility of determining the relevant scattering mechanisms in disordered graphene layers.

Now we compare the calculated scattering time ratio of graphene with the scattering time ratio of a normal 2D electron system with parabolic energy dispersion. We have the scattering time ratio for charged impurity (see Appendix A) in a normal 2D layer as

$$\frac{\tau_{tc}}{\tau_{sc}} = \begin{cases} \frac{1}{\pi r_s} - \frac{4}{\pi^2} \ln(r_s) & \text{for } r_s \ll 1 \\ 1 + \frac{4}{3\pi} \frac{1}{r_s} & \text{for } r_s \gg 1 \end{cases}, \quad (20)$$

where $r_s = 1/a_B \sqrt{\pi n}$ (a_B is an effective Bohr radius of the system and n is a carrier density). Unlike graphene, in normal 2D systems r_s depends on the carrier density. In small r_s (or high density) limit the ratio shows the same leading order behavior as graphene (i.e. $\tau_t/\tau_s \propto 1/r_s$), but in large r_s (low density) limit $\tau_t/\tau_s \rightarrow 1$. The difference between normal 2D system and graphene in the strong screening limit can be traced back to the suppression of the backscattering in graphene. We also find the difference in the scattering time ratio for short-ranged impurity. The ratio becomes $2/3 \leq \tau_{t\delta}/\tau_{s\delta} \leq 1$. (See Fig. 1 and Appendix A.) Thus, the ratio is always less than 1. In experiment, the ratio of the transport time to the single particle time has been found to be smaller than 1 in Si-MOSFET systems. Thus, in Si-MOSFET system the short-ranged scattering (such as interface roughness scattering) dominates.

It is, in principle, possible for the charged impurities to be at a distance “ z_i ” away from the 2D graphene layer. In fact, in 2D modulation doped GaAs-AlGaAs semiconductor heterostructures the charged dopants are put at a distance $d(\equiv z_i)$ away (inside the GaAlAs insulating barrier region) from the 2D electron gas in order to minimize the degradation of the electron mobility due to remote dopant scattering. As discussed in Sec. I of this paper, a large separation ($k_F z_i > 1$) leads to a very strong enhancement of the τ_t/τ_s in the GaAs-GaAlAs heterostructure since large-angle scattering by the remote impurities is strongly suppressed by the separation. To see the effect of separating the impurities from the graphene layer, all we need to do is to modify the form of the q -space Fourier transform of the electron-impurity Coulomb interaction by the factor e^{-qz_i} arising from the separation between the 2D carriers in the graphene layer and the charged impurity centers, leading to $V_{ei}(q, z_i) = V_{ei}(q)e^{-qz_i}$. With this simple modification for V_{ei} we can calculate the results for τ_t and τ_s for remote scatterers using the same formalism as above.

In Figs. 1–4 we present our theoretical results for τ_t/τ_s as well as τ_t and τ_s individually in graphene comparing it with the corresponding regular 2D results (i.e. non-chiral 2D electron system with parabolic band dispersion). We use exactly the same materials parameters for both graphene and the regular parabolic 2D system.

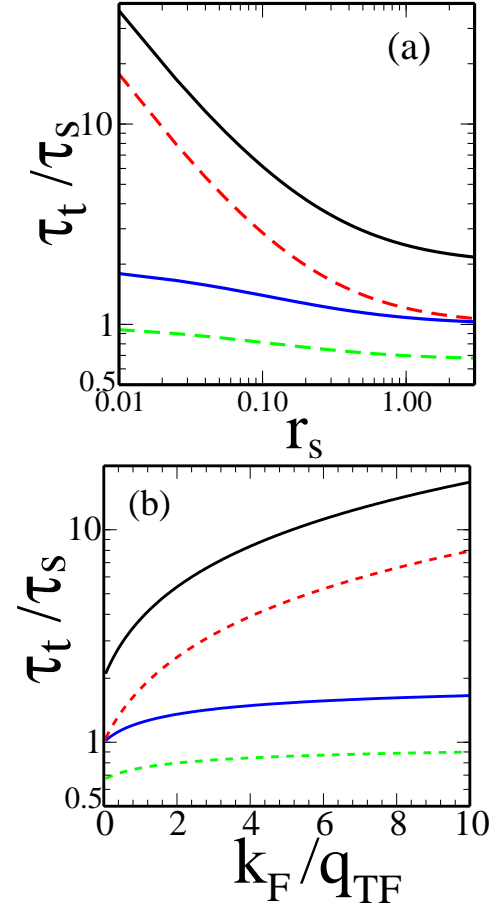


FIG. 1: (Color online) Calculated the ratio of the transport scattering time to single particle scattering time τ_t/τ_s (a) as a function of the parameter $r_s = e^2/\gamma\kappa$ and (b) as a function of k_F/q_{TF} . Top (bottom) solid line represents the ratio for charged impurity (short-ranged neutral impurity) scattering. Top (bottom) dashed line represents the ratio of normal 2D system with parabolic dispersion for charged impurity (short-ranged neutral impurity) scattering. We note that for graphene $k_F/q_{TF} \equiv 1/4r_s$.

The results are plotted as a function of the dimensionless parameter r_s (or k_F/q_{TF}), the impurity location from the interface z_i , or the density n where k_F (q_{TF}) are respectively the Fermi wave vector (Thomas-Fermi wave vector) for the system. We give the expressions for k_F and q_{TF} (with g as the spin and valley degeneracy factor): $k_F = (4\pi n/g)^{1/2}$ for both graphene and parabolic 2D systems, $q_{TF} = ge^2 k_F/(\kappa v_F)$ for graphene and $q_{TF} = gme^2/(\kappa\hbar^2)$ for 2D parabolic systems. We note that $q_{TF}/k_F = r_s$ for $g = 1$ and $q_{TF}/k_F \propto r_s$ for any value of g for both graphene and parabolic 2D systems. (In general, $g = 4$ for graphene.)

The most important qualitative feature of Figs. 1–2 is that in general τ_t/τ_s is larger in graphene than in the corresponding 2D parabolic system for all values of z_i including $z_i = 0$ (i.e. when the impurities are right at the substrate-2D layer interface). For $z_i \approx 0$ and for $r_s \approx 1$,

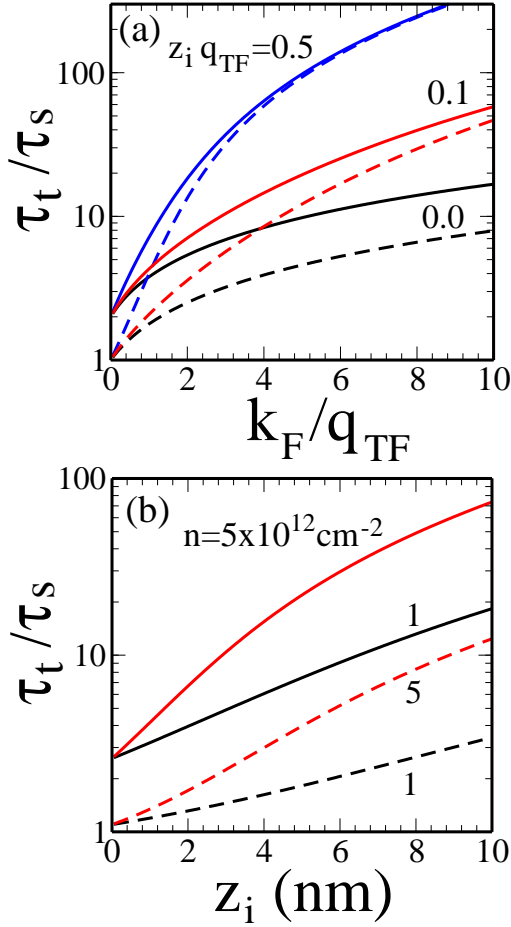


FIG. 2: (Color online) (a) The ratio τ_t/τ_s of graphene (with substrate SiO_2 , corresponding to $r_s = 0.9$) as a function of k_F/q_{TF} for different values of the separation z_i between the electron layer and the impurity layer. We use the dimensionless quantity $z_i q_{TF} = 0, 0.1, 0.5$. Solid (dashed) lines indicate results for graphene (normal 2D system). (b) The same as Fig. 2(a) as a function of z_i for two different electron densities, $n = 1, 5 \times 10^{12} \text{ cm}^{-2}$. Solid (dashed) line denote the results for charged Coulomb impurity (short-ranged neutral impurity).

the situation of current interest in graphene where the impurities are thought to be within $\sim 1 \text{ nm}$ of the interface (and the substrate is usually SiO_2), we get $\tau_t/\tau_s \sim 2$ in graphene although it is expected to increase fast with increasing z_i . We therefore suggest a measurement of τ_t/τ_s as a spectroscopic tool for the determination of the location of the impurity centers in graphene. It is interesting to note that in general $(\tau_t/\tau_s)_{\text{graphene}} > (\tau_t/\tau_s)_{2D}$ with the difference between them increasing sharply with increasing k_F/q_{TF} or z_i .

In Fig. 3 we show our calculated graphene transport and single particle times individually as a function of carrier density for various values of the impurity location z_i . In Fig. 3(a) where charged impurity Coulomb scattering is involved, both τ_t and τ_s increase with carrier density, but τ_t increases much faster, making τ_t/τ_s increase with

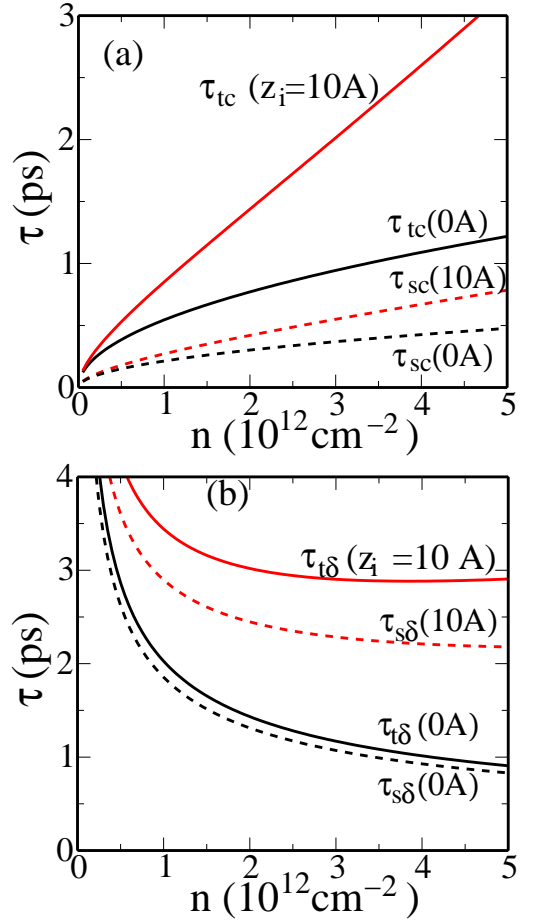


FIG. 3: (Color online) (a) Scattering times (in ps) of graphene (with substrate SiO_2) as a function of electron density for two different impurity locations $z_i = 0, 10 \text{ \AA}$. τ_{tc} (τ_{sc}) indicates the transport scattering time (single particle relaxation time) for Coulomb impurity scattering. We use an impurity density $n_{ic} = 10^{12} \text{ cm}^{-2}$. The same as Fig. 3(a) for a neutral impurity scattering. We use an impurity density $n_{i\delta} = 2 \times 10^{11} \text{ cm}^{-2}$ and $v_0 = 1 \text{ KeV \AA}^2$.

increasing density. But for short-range scattering (Fig. 3(b)), the reverse is true with both τ_t and τ_s decreasing with increasing density, but τ_s decreasing faster, again leading to an increasing τ_t/τ_s with increasing carrier density.

Finally, in Fig. 4 we show our calculated level broadening $\Gamma = \hbar/2\tau_s$ as a function of carrier density in graphene. We note that for charged impurity scattering Γ/E_F decreases monotonically with increasing carrier density. However, the scaled damping rate due to short-ranged impurity scattering is independent of the carrier density.

III. DISCUSSION AND CONCLUSION

We calculate the transport scattering time (τ_t) and the single particle relaxation time (τ_s) for disordered

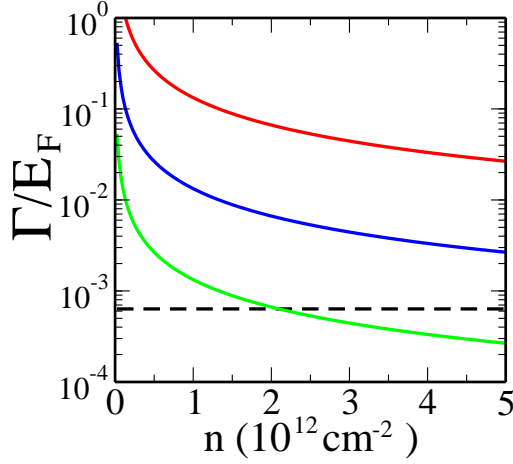


FIG. 4: (Color online) Calculated damping rates scaled by Fermi energy Γ/E_F as a function of carrier density for $r_s = 0.9$ which corresponds to graphene sample with SiO_2 substrate. Solid lines indicate damping rates due to charged impurity scattering with impurity density $n_{ic} = 100, 10, 1 \times 10^{10} \text{ cm}^{-2}$ (from top to bottom), respectively. Dashed line indicate a damping rate due to short-ranged impurity with impurity density $n_{id} = 10^{10} \text{ cm}^{-2}$ and potential strength $v_0 = 1 \text{ KeV } \text{\AA}^2$. We define $\Gamma = \hbar/2\tau_s$.

graphene in the lowest order of the electron-impurity interaction (Born approximation). The scattering mechanisms which we consider are screened charged impurity scattering and short-range potential (e.g. caused by lattice defects). For the screening function we use the RPA. We find that for short ranged scatterers, the ratio of the scattering time to the single particle relaxation time is always smaller than 2, but for charged impurity scattering, the ratio is always greater than 2. These theoretical results provide a technique to experimentally discriminate between short-range and Coulomb scattering as to the relevant scattering mechanism in disordered graphene layers. We also find a strong dependence of the ratio τ_t/τ_s in graphene on z_i the separation of the impurities from the 2D graphene layer. Somewhat surprisingly the dependence of τ_t/τ_s on z_i is stranger in graphene than in the corresponding parabolic 2D system, leading to the possibility that an accurate measurement of τ_t/τ_s in graphene could lead to better understanding of the impurity location underlying graphene disorder. In particular, τ_t/τ_s increases rapidly with increasing z_i in graphene (similar to non-chiral 2D GaAs-GaAlAs modulation doped heterostructure) and this could be directly experimentally tested.

We conclude by emphasizing that independent measurements of τ_t and τ_s in graphene samples could lead to detailed useful insight into the nature of disorder scattering of graphene carriers.

Acknowledgments

This work is supported by U.S. ONR, NSF-NRI, and SWAN.

APPENDIX A

Here we provide the scattering times of a normal 2D system with parabolic band. Using 2D RPA screening function¹² at $T = 0$ we have the scattering times for charged impurity centers

$$\frac{1}{\tau_{tc}} = \frac{1}{\tau_{0c}} I_{tc}(q_0), \quad (\text{A1a})$$

$$\frac{1}{\tau_{sc}} = \frac{1}{\tau_{0c}} I_{sc}(q_0), \quad (\text{A1b})$$

where

$$\frac{1}{\tau_{0c}} = 2\pi\hbar \frac{n_{ic}}{m} \left(\frac{2}{g}\right)^2 q_0^2, \quad (\text{A2})$$

n_{ic} is the density of charged impurity, $q_0 = q_{TF}/2k_F$ ($q_{TF} = g/a_B$ is a 2D Thomas-Fermi wave vector with effective Bohr radius $a_B = \hbar^2/me^2$), and $I_{tc}(q_0)$, $I_{sc}(q_0)$ are given by

$$I_{tc}(q_0) = \pi - 2 \frac{d}{dq_0} [q_0^2 f(q_0)] \quad (\text{A3})$$

$$I_{sc}(q_0) = - \frac{d}{dq_0} f(q_0) \quad (\text{A4})$$

where $f(x)$ is given in Eq. (12) and its derivative is given by

$$\frac{df}{dx} = \frac{1}{x} \frac{1}{x^2 - 1} [1 - x^2 f(x)] \quad (\text{A5})$$

For short-ranged impurity centers we have

$$\frac{1}{\tau_{t\delta}} = \frac{1}{\tau_{0\delta}} I_{t\delta}(q_0), \quad (\text{A6a})$$

$$\frac{1}{\tau_{s\delta}} = \frac{1}{\tau_{0\delta}} I_{s\delta}(q_0), \quad (\text{A6b})$$

where

$$\frac{1}{\tau_{0\delta}} = \frac{2n_{i\delta}}{\pi\hbar^3} m v_0^2, \quad (\text{A7})$$

$n_{i\delta}$ is the density of short-ranged impurity, $n_{i\delta}$, v_0 is the potential strength and $I_{t\delta}(q_0)$, $I_{s\delta}(q_0)$ are given by

$$I_{t\delta}(q_0) = \frac{\pi}{2} - 4q_0 + 3\pi q_0^2 - 2 \frac{d}{dq_0} [q_0^4 f(q_0)] \quad (\text{A8})$$

$$I_{s\delta}(q_0) = \frac{\pi}{2} - \frac{d}{dq_0} [q_0^2 f(q_0)]. \quad (\text{A9})$$

-
- ¹ S. Das Sarma and F. Stern, Phys. Rev. B **32**, 8442 (1985).
 - ² S. Das Sarma, A. K. Geim, P. Kim, and A. H. MacDonald, eds., *Exploring Graphene: Recent Research Advances, A Special Issue of Solid State Communications*, vol. 143 (Elsevier, 2007).
 - ³ T. Ando, J. Phys. Soc. Jpn. **75**, 074716 (2006).
 - ⁴ V. V. Cheianov and V. I. Fal'ko, Phys. Rev. Lett. **97**, 226801 (2006).
 - ⁵ K. Nomura and A. H. MacDonald, Phys. Rev. Lett. **98**, 076602 (2007).
 - ⁶ E. H. Hwang, S. Adam, and S. Das Sarma, Phys. Rev. Lett. **98**, 186806 (2007) (2007).
 - ⁷ S. Adam, E. H. Hwang, V. Galitski, and S. Das Sarma, Proc. Natl. Acad. Sci. USA **104**, 18392 (2007).
 - ⁸ Y.-W. Tan, Y. Zhang, K. Bolotin, Y. Zhao, S. Adam, E.H. Hwang, S. Das Sarma, H. L. Stormer, and P. Kim, Phys. Rev. Lett. **99**, 246803 (2007).
 - ⁹ J. H. Chen, C. Jang, M. S. Fuhrer, E. D. Williams, and M. Ishigami, arXiv:0708.2408.
 - ¹⁰ J. P. Harrang, R. J. Higgins, R. K. Goodall, P. R. Jay, M. Laviro, and P. Delescluse, Phys. Rev. B **32**, 8126 (1985); R. G. Mani and J. R. Anderson, Phys. Rev. B **37**, 4299 (1988); M. Sakowicz, J. Lusakowski, K. Karpierz, M. Grynberg, and B. Majkusiak, App. Phys. Lett. **90**, 172104 (2007).
 - ¹¹ E. H. Hwang and S. Das Sarma, Phys. Rev. B **75**, 205418 (2007) (2007).
 - ¹² T. Ando, A. B. Fowler, and F. Stern, Rev. Mod. Phys. **54**, 437 (1982).
 - ¹³ S. Das Sarma and B. Vinter, Phys. Rev. B **24**, 549 (1981).